Jan Cox, Lea Marie Esser, Maximilian Jüdt, Katharina Schmitz, Kaja Reiffert, Matthias Grimmler, Björn Stork, Sebastian Wesselborg and Christoph Peter*

NF90/NFAR (nuclear factors associated with dsRNA) – a new methylation substrate of the PRMT5-WD45-RioK1 complex

https://doi.org/10.1515/hsz-2022-0136
Received March 10, 2022; accepted August 12, 2022;
published online August 31, 2022

Abstract: Protein-arginine methylation is a common post-translational modification, crucial to various cellular processes, such as protein-protein interactions or binding to nucleic acids. The central enzyme of symmetric protein arginine methylation in mammals is the protein arginine methyltransferase 5 (PRMT5). While the methylation reaction itself is well understood, recruitment and differentiation among substrates remain less clear. One mechanism to regulate the diversity of PRMT5 substrate recognition is the mutual binding to the adaptor proteins pICln or RioK1. Here, we describe the specific interaction of Nuclear Factor 90 (NF90) with the PRMT5-WD45-RioK1 complex. We show for the first time that NF90 is symmetrically dimethylated by PRMT5 within the RG-rich region in its C-terminus. Since upregulation of PRMT5 is a hallmark of many cancer cells, the characterization of its dimethylation and modulation by specific commercial inhibitors *in vivo* presented here may contribute to a better understanding of PRMT5 function and its role in cancer.

Keywords: NF90; PRMT5; protein-arginine methylation; RioK1.

Introduction

Posttranslational modifications are an important mechanism to regulate the functions of cellular proteins. The methylation of nitrogen in the side chain of arginine is one of the most common modifications and plays an important role in a variety of cellular processes such as histone methylation, RNA splicing, transcription and translation regulation, nuclear export of proteins, and protein-protein interactions (Blanc and Richard 2017; Murn and Shi 2017). To date, more than 5500 human proteins have been detected to be methylated, highlighting the central function of this modification (Murn and Shi 2017). Three arginine methylation patterns are differentiated (Blanc and Richard 2017). Methylation of one nitrogen leads to an N^G-monomethyl arginine (MMA). If both nitrogen atoms are methylated, symmetrical dimethylation (SDMA) and asymmetrical dimethylation (ADMA) are differentiated. In SDMA, both nitrogen atoms are individually methylated, resulting in an N^G, N'^G-dimethylarginine. In ADMA, one of the two nitrogen atoms is double methylated, resulting in an N^G, N^G-dimethylarginine. Responsible for this kind of dual modification is the family of protein arginine methyltransferases (PRMTs), which transfer the methyl group of S-adenosylmethionine (SAM) onto the guanidine group in the side chain of arginine (Bedford and Clarke 2009). The methyltransferase PRMT5 is the only methyltransferase that catalyzes symmetric dimethylation of arginines *in vivo*. Consequently, the loss of PRMT5 leads to a nearly complete loss of SDMA (Hadjikyriacou et al. 2015). PRMT5 together with the WD repeat-containing protein 45 (WD45) forms a hetero-octameric complex of ~450 kDa (Antonysamy et al. 2012). This structure represents the basic core complex and can be extended by the adapter proteins pICln or RioK1, which regulate the substrate specificity of PRMT5 (Guderian et al. 2011; Krzyzanowski et al. 2021; Mulvaney et al. 2021).

Here, we identified the nucleic acid-binding protein NF90 as a novel substrate of the PRMT5/WD45/RioK1 complex. Strikingly, NF90 has RG-rich sequences in the C-terminus, representing potential PRMT5-dependent methylation sites, but no methylation has yet been shown. In this work, we demonstrate that NF90 is recruited exclusively via the adapter protein RioK1 to the PRMT5-WD45 complex, where it is rapidly methylated in its C-terminal region at the RG-boxes. In immunopurification studies, we further show that both

***Corresponding author: Christoph Peter**, Institute of Molecular Medicine I, Medical Faculty and University Hospital Düsseldorf, Heinrich Heine University Düsseldorf, D-40225 Düsseldorf, Germany, E-mail: christoph.peter@uni-duesseldorf.de
Jan Cox, Lea Marie Esser, Maximilian Jüdt, Katharina Schmitz, Kaja Reiffert, Björn Stork and Sebastian Wesselborg, Institute of Molecular Medicine I, Medical Faculty and University Hospital Düsseldorf, Heinrich Heine University Düsseldorf, D-40225 Düsseldorf, Germany
Matthias Grimmler, Hochschule Fresenius gGmbH, University of Applied Sciences, Limburger Straße 2, D-65510 Idstein, Germany; and DiaSys Diagnostic Systems GmbH, Alte Strasse 9, D-65558 Holzheim, Germany

endogenous NF90 and overexpressed NF90 are fully methylated in cells.

Results

NF90 interacts with the PRMT5/WD45/RioK1 complex

In previous work, NF90 was identified as a new potential interaction partner of the PRMT5/WD45/RioK1 complex by mass spectrometry (Guderian et al. 2011). In this follow-up study, we show that NF90 is indeed a binding partner and a new substrate of PRMT5 *in vitro* and *in vivo*. To investigate the complex composition and the recruitment of NF90, we generated cell lines, stably overexpressing PRMT5, WD45, pICln, and RioK1 as GFP fusion proteins. By immunoprecipitation studies, we observed co-immunoprecipitation of NF90 with GFP-PRMT5, GFP-WD45, and GFP-RioK1, whereas we could not precipitate NF90 with GFP-pICln (Figure 1A). Data by Guderian et al. showed, that the substrate specificity and recruitment of new substrates of PRMT5 are controlled by its adaptor proteins RioK1 or pICln (Guderian et al. 2011). NF90, predominantly purified by GFP-RioK1 but not by pICln, supports this model of regulating the mutual substrate specificity of PRMT5. Further pulldown experiments, utilizing heterologous expressed GST fusion proteins from *Escherichia coli*, confirmed these results: endogenous NF90 from HEK293 lysates bound to GST-RioK1 and GST-PRMT5 but not to GST-pICln (Figure 1B).

Interaction with the PRMT5/WD45/RioK1 complex occurs via the C-terminus of NF90

NF90 is a multi-domain protein consisting of two double-stranded RNA-binding motifs (DRBM), a domain

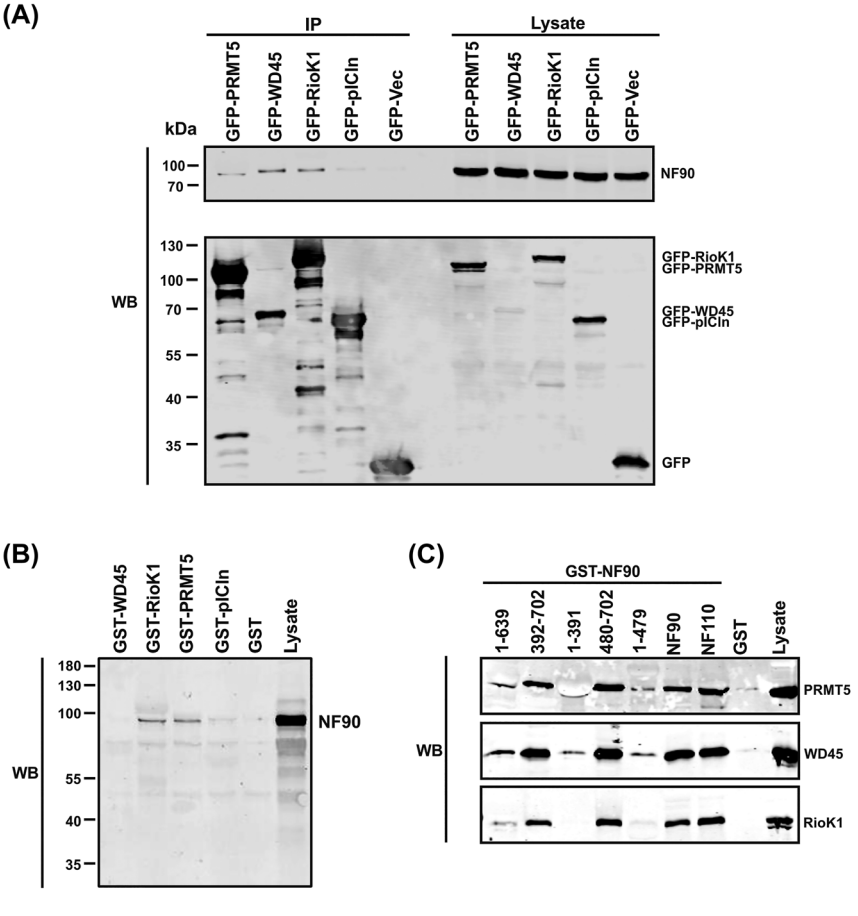

(D)

Dissociation constant (K_D)	RioK1	WD45	NF90	NF90+WD45	NF90+WD45+RioK1
GST-PRMT5	100 nM ±29 nM	622 nM ±251 nM	57 nM ±18 nM	68 nM ±22 nM	84 nM ±25 nM

Figure 1: NF90 interacts with the PRMT5/WD45/RioK1 complex.
(A) Immunoprecipitation from GFP-PRMT5, -WD45, -Riok1, -pICln, and GFP overexpressing cells. Protein expression was induced with 0.1 µg/mL doxycycline for 24 h and as input 25 µg of total protein was loaded. After cell lysis, GFP-IP was performed and analyzed by Tris/glycine-SDS-PAGE and Western blotting, using antibodies against GFP and NF90. NF90 was co-immunoprecipitated with GFP-PRMT5, GFP-WD45 and GFP-RioK1. (B) Pulldown assays with recombinant GST-PRMT5, -WD45, -pICln, -RioK1, and GST purified from *E. coli* were executed in HEK293 lysate overnight at 4 °C. Co-precipitation of NF90 was analyzed using NF90 antibody and was detectable for GST-RioK1 and GST-PRMT5. (C) Pulldown assay as described above with different truncated forms of GST-NF90 purified from *E. coli*. Detection of co-precipitated proteins was performed with RioK1, WD45, and PRMT5 antibodies. Only the C-terminus of NF90 interacts with RioK1, WD45, and PRMT5. (D) Interaction studies using microscale thermophoresis measurements (MST). GST-PRMT5 was labeled with AlexaFluor488 fluorescent dye and measured against the interaction partners RioK1, WD45, and NF90. GST-PRMT5 showed a high affinity to its substrate NF90 with 57 nM. WB: Western blotting.

associated with zinc fingers (DZF), a bipartite nuclear localization signal (NLS), and an RG-motif (see also Figure 2 C). Due to the multi-domain structure of NF90, we generated truncated forms of NF90 (Figure 2C) to characterize the interaction of NF90 with the proteins of the PRMT5/WD45/RioK1 complex in more detail (Figure 1C). To this end truncations of NF90 were generated by dividing the two DRBMs (NF90 aa1-479 and NF90 aa480-702) and also dividing between the DZF domain and both DRBMs (NF90 aa1-391 and NF90 aa392-702) (Figure 2C). Another truncated form represents NF90 without the RG-motif in the C-terminal region (NF90 aa1-639) (Figure 2C). Interaction studies based on these forms of NF90 revealed an interaction of the PRMT5/WD45/RioK1 complex with the C-terminal region of NF90 spanning from amino acid 392 to 702 (Figure 1C). Interestingly, the truncated form aa1-639, which represents almost the entire protein except for the RG-motif, showed only weak interaction. This indicates that the interaction predominantly occurs in the RG-rich region at the C-terminus of NF90 (Figure 1C and 2C). To determine the affinities among the components of the PRMT5 complex and with the substrate protein NF90,

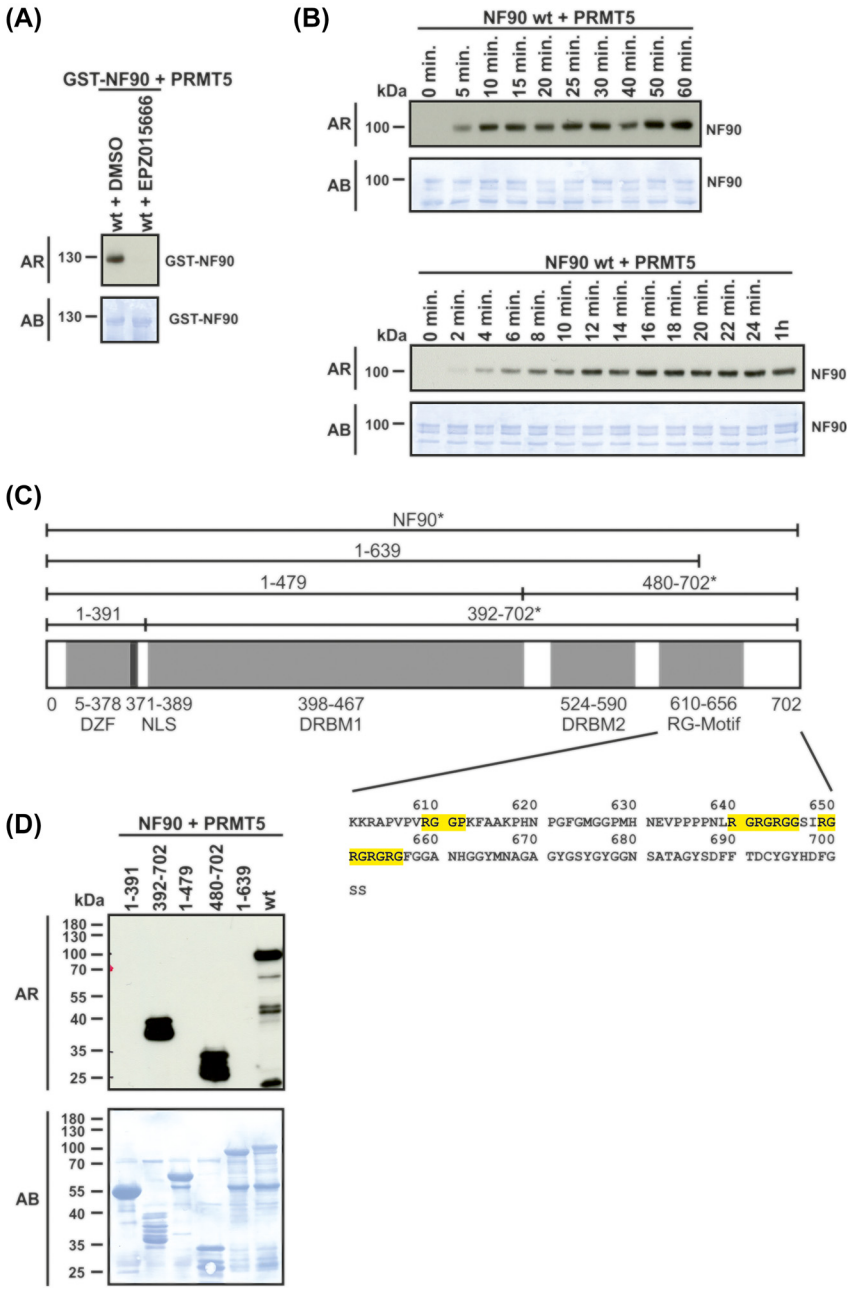

Figure 2: The C-terminus of NF90 is methylated by PRMT5.
(A) Radioactive *in vitro* methylation assay using GST-NF90 purified from *E. coli* and 200 ng recombinant PRMT5 and 1 µCi [3H]-SAM was performed with and without 1 mM PRMT5 inhibitor EPZ015666. Samples were separated by Tris/glycine-SDS-PAGE and radioactive incorporation was analyzed by Western blotting and autoradiography. The addition of 1 mM PRMT5 inhibitor EPZ015666 inhibits the methylation of NF90 by PRMT5. (B) Investigation of the time-dependent methylation of NF90. 880 ng NF90 purified from *E. coli* without GST-tag was incubated with 200 ng recombinant PRMT5 and 1 µCi [3H]-SAM. The reaction was terminated by addition of SDS sample buffer and the samples were analyzed as described in (A). (C) Schematic overview of the domains and truncated forms of NF90 used in this work. The asterisks indicate methylatable forms and the distinctive RG-boxes have been highlighted in yellow. (D) Methylation assay of truncated NF90 forms purified from *E. coli* as described in (A). NF90 is methylated in the C-terminus between amino acids 640 and 702 by PRMT5. AR: autoradiography, AB: amido black staining.

microscale thermophoresis experiments were performed. For this purpose, GST-PRMT5 was labeled with Alexa flour 488 fluorescent dye and first measured against the known interaction partners of the complex, RioK1 and WD45. PRMT5 showed a strong affinity for RioK1 with a K_D of 100 nM and still a strong attachment to WD45 with a K_D of 622 nM (Figure 1D, Supplementary Figure 1). In contrast, the affinity of the substrate protein NF90 towards the methyltransferase PRMT5 was determined with a high affinity of 57 nM (Figure 1D, Supplementary Figure 1). Only marginal changes of affinity could be observed if WD45 was added or WD45 and RioK1 in combination. The data so far lead to the assumption that NF90 is a strong binding partner of PRMT5 *in vitro* and that substrate binding directly occurs to PRMT5 by the RG-rich stretch of NF90.

NF90 is a new substrate of PRMT5

Based on this strong *in vitro* interaction, we performed radioactive *in vitro* methylation assays with recombinant NF90 and active PRMT5 to test whether NF90 is methylated by PRMT5. Indeed, the radioactive methyl group from [3H]-SAM was transferred to GST-NF90 (Figure 2A). Treatment with the PRMT5-specific inhibitor EPZ015666 did not result in radioactive incorporation (Chan-Penebre et al. 2015). Both experiments prove that NF90 is symmetrically methylated by PRMT5 *in vitro* (Figure 2A).

To assess the kinetics of NF90 methylation, we performed a titration of the methylation reaction. As evident in Figure 2B, a saturation of NF90 methylation did occur already within 10 min. To gain a more detailed view on the methylation dynamics of NF90, 2 min steps, up to 24 min were performed. Again, no increase in methylation could be observed after 12 min (Figure 2B). The NF90 protein contains several putative methylation sites (arginine-glycine-repeats, RG-Box) in the C-terminus between the amino acids 609 to 656. To further determine the location of the methylation sites within the NF90 protein we analyzed truncated forms (Figure 2D) by methylation assays. We identified eight arginine residues as potential targets in this region (Figure 2C, highlighted in yellow), in particular, we observed methylation of the C-terminal forms NF90 aa392-702 and NF90 aa480-702 and the wild-type NF90 protein (Figure 2D). In contrast, no methylation was observed for the N-terminal forms NF90 aa1-391, NF90 aa1-479, and NF90-aa1-639 (Figure 2D). These results clearly show methylation of NF90 by PRMT5 exclusively is located within the C-terminal RG-rich sequence ranging from amino acid 640 to 702.

NF90 is methylated *in vivo* by PRMT5 in an RG-rich region in the C-terminus

Based on these data, we focused on the RG-motif in the C-terminal region of NF90 in more detail. This RG-rich region contains seven glycine-arginine residues that potentially may serve as methylatable residues to PRMT5 (Figure 2C). All arginines in the RG-rich region of NF90 at positions 640, 642, 644, 649, 651, 653, and 655 were exchanged to the structurally similar but non-methylatable lysines. The obtained methylation deficient mutant (NF90-7x R-to-K) and the NF90 wildtype protein were expressed in *E. coli* and the purified recombinant proteins were subsequently analyzed by methylation assays (Figure 3A). In contrast to wild-type NF90, no methylation could be detected in the methylation-deficient mutant, indicating that the methylation sites are located in the region of amino acids 640 to 655 in the C-terminus of NF90.

Next, we investigated the intracellular methylation status of endogenous NF90 from HEK cells. For this purpose, we immunoprecipitated endogenous NF90 from HEK cells and used it as a substrate for an *in vitro* methylation assay. However, endogenous NF90 showed no incorporation of radioactive 3H (Figure 3B), leading to the assumption, that NF90 is already completely methylated *in vivo*. To substantiate this hypothesis, HEK293 cells were treated with 20 μM adenosine dialdehyde (Adox) to disable endogenous methylation, before the respective cell extract was subjected to immunoprecipitation of NF90. Adox is a well-known broad inhibitor of methyltransferases (Chen et al. 2004). In consequence, newly synthesized proteins remain hypomethylated upon Adox treatment (Chen et al. 2004) and therefore are receptive for *in vitro* methylation if purified from the respective extracts. By using immunoprecipitated endogenous NF90 with and without treatment by Adox, we clearly could show methylation by Adox treated NF90, but not by DMSO/control-treated NF90 upon incubation with recombinant PRMT5 (Figure 3B). To this point, treatment of HEK293 cells with Adox does not alter NF90 cellular expression nor efficiency of immunoprecipitation (Figure 3B) but does alter endogenous methylation status of NF90. Upon the observed rate of methylation of Adox pretreated NF90 substrate protein, endogenous NF90 probably is fully methylated in the cell under normal conditions. To prove this finding, we repeated the experiments with HEK293 Flp-In T-REx cell lines inducibly overexpressing NF90 wildtype as a GFP-fusion protein (GFP-NF90 wt) or the methylation-deficient GFP-NF90 7x mutant (Figure 3C). First, the intracellular protein methylation was blocked by Adox treatment, and

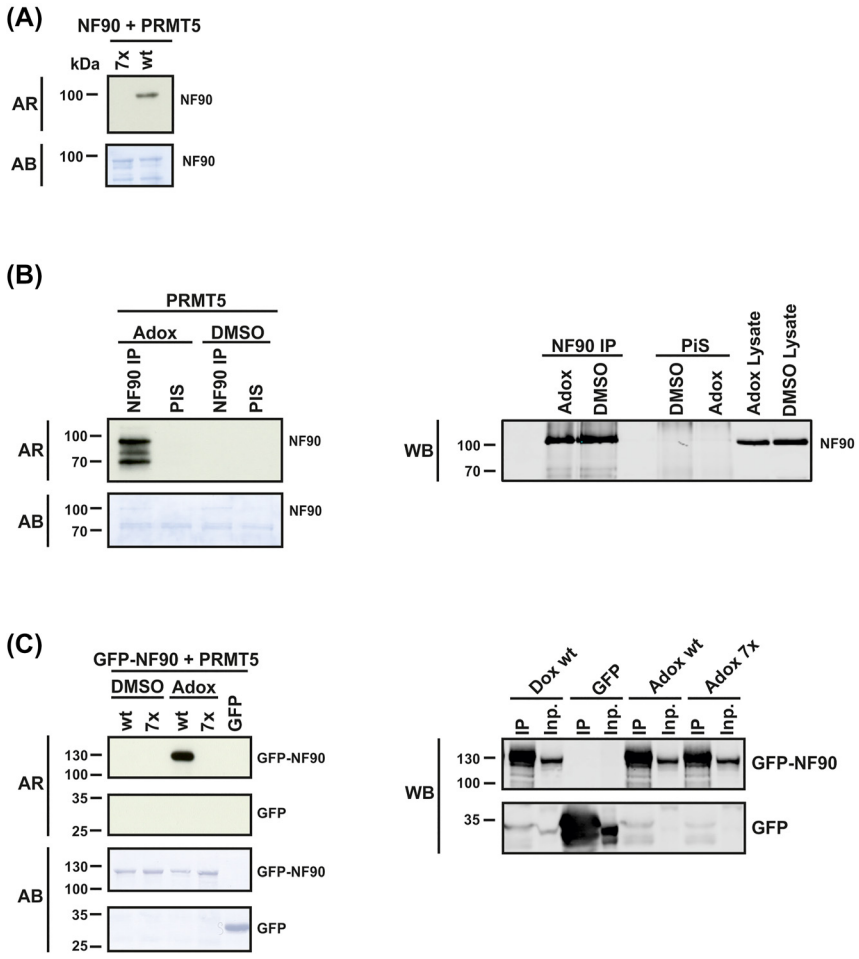

Figure 3: NF90 arginine mutants and *in vivo* inhibitor studies.
(A) Recombinant NF90 wt, and NF90 7x from *E. coli* was incubated with 200 ng recombinant PRMT5 and 1 µCi [3-H]-SAM. Samples were separated by Tris/glycine-SDS-PAGE and radioactive incorporation was analyzed by Western blotting and autoradiography. In the NF90 7x mutant, all seven potential arginine methylation sites are mutated to lysines (see Figure 2C). PRMT5 was not able to methylate the sevenfold arginine to lysine mutant. (B) HEK293 cells were treated with 20 µM of the S-adenosylmethionine-dependent methyltransferase inhibitor adenosine dialdehyde (Adox). 500 µg lysate with 1 µg NF90 antibody or as control Preimmunserum (PIS) and Protein G Sepharose was incubated for 1.5 h and immunopurified NF90 was subjected to a methylation assay as described in (A). Only NF90 from Adox-treated cells could be methylated *in vitro*. (C) Flp-In T-REx 293 cells stably expressing GFP-NF90 wt and GFP-NF90 7x were stimulated with 0.1 µg/mL doxycycline for 24 h and treated with Adox as described in (B). After GFP-IP, a methylation assay was performed. No methylation of purified GFP-NF90 occurred in control cells (DMSO), whereas NF90 immunopurified from cells treated with Adox could be methylated *in vitro*. The sevenfold lysine mutant GFP-NF90 7x showed no methylation in all conditions. AR: autoradiography, AB: amido black staining, WB: Western blotting.

subsequently, NF90 protein expression was induced. GFP-immunoprecipitations allowed for exclusive precipitation and measurement of newly synthesized NF90, excluding endogenous, untagged NF90. Again, no methylation of purified GFP-NF90 occurred in control cells (DMSO), whereas NF90 from Adox treated cells could be methylated *in vitro* (Figure 3C). Taken together, these experiments indicate that endogenous as well as overexpressed NF90 are completely methylated in the normal cellular setting.

Discussion

Although the RG-motif of NF90 has been postulated as a potential methylation site by PRMT5 (Richard et al. 2005), no methylation has yet been detected. In this work, we describe for the first time NF90 as a new interaction partner of the PRMT5/WD45/RioK1 complex and as a new symmetrically methylated substrate of the methyltransferase PRMT5.

Due to the ability of RioK1 to bind numerous proteins containing RG-motifs, it increases the substrate diversity of PRMT5 and recruits new substrates to the methyltransferase (Guderian et al. 2011). Here, we observed NF90 co-immunoprecipitation within the PRMT5/RioK1 complex but not with pICln (Figure 1A and B). These data confirm that NF90 recruitment occurs only via the RioK1-containing complex and not via pICln. For this, NF90 is a novel interaction partner of the PRMT5/WD45/RioK1 complex. Moreover, the C-terminal region of NF90 (aa 640 – 702) was identified as the interaction surface with this complex (Figure 1C). The determined dissociation constant (K_D) of 100 ± 29 nM within the protein complex for RioK1 and PRMT5 (Figure 1D) matches to 34 nM, reported in previous studies (Krzyzanowski et al. 2021). A dissociation constant of 57 ± 18 nM was observed for PRMT5 and NF90, indicating a high affinity of PRMT5 for NF90. The addition of RioK1 did not significantly alter the dissociation constants, nor did it affect NF90 methylation, as recombinant NF90 is methylated just as rapidly in the presence or absence of RioK1 under *in vitro* conditions (Figure 2B and Supplementary Figure 2A). Also, *in vitro* methylation experiments with the SmB protein show that under these conditions methylation can occur independently of pICln (Supplementary Figure 2B). This is in line with the results of previous studies, which described a direct enzyme-substrate interaction for PRMT5 to its substrates histones H2A, H3, and the myelin basic protein (Pal et al. 2004; Pollack et al. 1999).

However, for recruiting NF90 to the PRMT5 complex in the cell, the adapter protein RioK1 may play an essential role like pICln for the Sm proteins. The specific role of PRMT5 adapter proteins (e.g. pICln and RioK1) to regulate substrate specificity of methyltransferases is a very important and exciting question. Recent approaches to answer this question aim to develop novel inhibitors for the adapter proteins and thus identify adapter protein-dependent as well as independent substrates and thus also control the activity of PRMT5 concerning targeted substrates (Krzyzanowski et al. 2021; Mckinney et al. 2021; Mulvaney et al. 2021). As both proteins, NF90 and PRMT5, attribute a crucial function in ribosome biosynthesis a cooperative function of both proteins at the ribosome is conceivable (Wandrey et al. 2015; Widmann et al. 2012). To gain complete functionality in ribosome biosynthesis NF90 may require full methylation. To this end, RioK1 may recruit PRMT5 towards the ribosome for this purpose. RioK1 in this scenario attributes a comparable role as pICln does in recruiting Sm proteins during snRNP biogenesis (Chari et al. 2008; Schmitz et al. 2021).

Investigation of the protein sequence of NF90 showed that there is a glycine-arginine-rich (GAR) motif in the C-terminal region. GAR motifs are described as a consensus sequence of protein methylation (Lapeyre et al. 1986) and GR repeats that have glycine at position –1 are predominantly methylated by PRMT5 (Musiani et al. 2019). In the C-terminal region of NF90, the sequence "R^{640}GRGRGGSI RGRGRGRGF^{657}" contains a triple RG repetition followed by a quadruple RG repetition sequence, flanked by glycines (Figure 2C).

So far, the methylation status of NF90 *in vivo* was unclear. We observed that immunoprecipitated NF90 could not be methylated in an *in vitro* methylation assay by recombinant PRMT5 (Figure 3B). As evident by Adox treatment (Figure 3B), endogenous NF90 is predominantly present as a hypermethylated protein since subsequent efficient methylation of immunoprecipitated NF90 by PRMT5 was possible. The treatment of cells by Adox results in a loss of methyl groups in newly formed proteins and free methylation sites, capably to be methylated in a subsequent *in vitro* methylation assay of respective precipitated substrate proteins. Also beforehand *in vitro* investigations based on the NF90 7x mutant (Figure 3A and C) confirmed the exclusive methylation of the seven arginine residues in the C-terminus of NF90 *in vivo* hence by Adox treatment, no methylation of this mutant could be observed. This observation also clearly excludes other PRMT5-specific arginine methylation sites of NF90, for example at positions 90, 247, 537, or 609. Strikingly, even when strongly overexpressed in HEK293 cells, GFP-NF90 wt is completely methylated (Figure 3C). This finding as well as rapid methylation of NF90 (Figure 2B) implies the stringency of the cell's methylation system and supports a general necessity for complete methylation of NF90 *in vivo* (Figure 3C). In this work, we prove that NF90 is fully methylated in the cell under normal conditions and does not harbor any free methyl acceptor sites. These results are well supported by earlier work, which also described almost complete methylation of proteins, such as heterogeneous nuclear ribonucleoprotein U (hnRNP U) (Herrmann et al. 2004), nucleolin, or fibrillarin (Lischwe et al. 1982, 1985).

Currently, it is assumed that symmetric methylation of NF90 is irreversible and persists throughout the lifetime of the protein. Little is known about demethylases but the Jumonji domain-containing 6 protein (JMJD6) was described as arginine demethylase (Chang et al. 2007). However, the results could not be reproduced in other studies (Han et al. 2012; Webby et al. 2009) whereas arginine demethylation activity was observed in recent studies (Liu et al. 2013; Poulard et al. 2014; Tsai et al. 2017). Therefore, arginine demethylation by JMJD6 remains highly controversial (Bottger et al. 2015). This raises the question of the biological function of irreversible

methylation of NF90. Since many proteins have more than one methylation site but demethylation reactions have rarely been observed and are critically viewed, a regulatory function through turnover as in phosphorylation is unlikely (Herrmann et al. 2004; Simms et al. 1987). However, the production of SAM certainly consumes ATP and the cell does not make this effort unnecessarily in NF90.

It will be interesting in further studies to investigate the impact of the methylation of NF90 discovered here in this work in terms of functionality, as NF90 is a protein involved in a variety of signaling cascades.

Materials and methods

Cloning and plasmids

NF90 (CCDS12247.1) cDNA was generated from HEK293 cells with cDNA Transcription Kit (4,368,814, Applied Biosystems) and cloned into pGEX-6P-1 (28,954,648, Cytiva) and pcDNA5-FRT-TO (V601020, Invitrogen) using Gibson assembly (NEB, E2621S) or restriction enzyme cloning. Phusion Polymerase (M0530, NEB) and the following primers (Sigma-Aldrich) were used:

pGEX-6P-1-NF90 wt, 5′-GTGAATTCATGCGTCCAATGCGAATT-3′
and 5′-GTGCGGCCGCCTAGGAAGACCCAAAATCATGAT-3’;
pGEX-6P-1-NF90AA1-639,
5′-CACAAGAGGAGCTGGAGGCAGTCCAGAACATGGTG-3′
and 5′- TCCAGCTCCTCTTGTGTTGGATAAACGGAAGAATG-3′
and 5′-AACCTTTAGGCGGCCGCATCGTGACTGACTG-3′
and 5′-CGGCCGCCTAAAGGTTGGGGGGTGGGGGCAC-3’;
pGEX-6P-1-NF90 AA1-479, 5′-GTGAATTCATGCGTCCAATGCGAATT-3′
and 5′-GTGCGGCCGCCCCCTTGCTCGAGTCC-3’;
pGEX-6P-1-NF90 AA480-702, 5′-GTGAATTCGAGGACTCGGCTGAGGAG-3′
and 5′-GTGCGGCCGCCTAGGAAGACCCAAAATCATGAT-3’;
pGEX-6P-1-NF90 AA1-391, 5′-GTGAATTCATGCGTCCAATGCGAATT-3′
and 5′-GTGCGGCCGCCTACTGAATCTTCTTCTTCTTTTTGCTG-3’;
pGEX-6P-1-NF90 AA392-702, 5′-GTGAATTCAAGAAAGAGGAGAAGGCAGAG-3′
and 5′-GTGCGGCCGCCTAGGAAGACCCAAAATCATGAT-3’;
pGEX-6P-1-NF90 AA609 R->K, 5′-AGCCCCAGTACCCGTCAAAGGGGGACC-3′
and 5′-GGTCCCCCTTTGACGGGTACTGGGGCT-3’;
pGEX-6P-1-NF90 7x AA640, 642, 644, 649, 651, 653, 655 R->K (GeneArt Gene Synthesis, Invitrogen);
pGEX-6P-1-NF90 AA640 R->K,
5′-CCCCAACCTTAAAGGGCGGGGAAGAGGCGGGAG-3′
and 5′-CCCCGCCCTTTAAGGTTGGGGGGTGGGGGCAC-3’;
pGEX-6P-1-NF90 AA642 R->K,
5′-TCGAGGGAAGGGAAGAGGCGGGAGCATCCGGGGAC-3′
and 5′-CCGCCTCTTCCCTTCCCTCGAAGGTTGGGGGGTGG-3’;
pGEX-6P-1-NF90 AA644 R->K,
5′-TCGAGGGCGGGGAAAAGGCGGGAGCATCCGGGGAC-3′
and 5′-CCGCCTTTTCCCCGCCCTCGAAGGTTGGGGGGTG-3’;
pGEX-6P-1-NF90 AA649 R->K,
5′-AGGCGGGAGCATCAAGGGACGAGGGCGCGGGCGAG-3′
and 5′-CGTCCCTTGATGCTCCCGCCTCTTCCCCGCCCTC-3’;
pGEX-6P-1-NF90 AA651 R->K,
5′-ATCCGGGGAAAAGGGCGCGGGCGAGGATTTGG-3′
and 5′-CCCGCGCCCTTTTCCCCGGATGCTCCCGCCTC-3’;
pGEX-6P-1-NF90 AA653 R->K,
5′-ACGAGGGAAGGGGCGAGGATTTGGTGGCGCCAAC-3′
and 5′-AATCCTCGCCCCTTCCCTCGTCCCCGGATGCTCC-3’;
pGEX-6P-1-NF90 AA655 R->K,
5′-GGGCGCGGGAAAGGATTTGGTGGCGCCAACCATGG-3′
and 5′-ACCAAATCCTTTCCCGCGCCCTCGTCCCCGGATG-3’.

Plasmids:

pcDNA5-FRT-TO-NF90 wt, pcDNA5-FRT-TO-NF90 AA640, 642, 644, 649, 651, 653, 655 R->K (7x), 5′-ATGCGTCCAATGCGAATTTTTGTGAATGATGAC-3′
and 5′-TCGCATTGGACGCATGGATCCGAGCTCGGTACCAAGC-3′
and 5′-TTTGGGTCTTCCTAGGCGGCCGCTCGAGTCTAGAGG-3′
and 5′-CTAGGAAGACCCAAAATCATGATAGCCGTAG-3’;
pcDNA5-FRT-TO-eGFP-NF90 wt and pcDNA5-FRT-TO-eGFP-NF90 AA640, 642, 644, 649, 651, 653, 655 R->K (7x),
5′-ATCCATGCGTCCAATGCGAATTTTTGTGAATGATGAC-3′
and 5′-CATTGGACGCATGGATCCGAGTCCGGACTTGTACAG-3′
and 5′-TTTGGGTCTTCCTAGGCGGCCGCTCGAGTCTAGAGG-3′
and 5′-CTAGGAAGACCCAAAATCATGATAGCCGTAG-3’;
pcDNA5-FRT-TO-eGFP-PRMT5,
5′-GGATCCATGGCGGCGATGGCGGT-3′
and 5′-GCGGCCGCCTAGAGGCCAATGGTATAT-3’;
pcDNA5-FRT-TO-eGFP-RioK1,
5′-GGATCCATGGACTACCGGCGGCTTC-3′
and 5′-GCGGCCGCCTATTTGCCTTTTTTCGTCT-3’;
pcDNA5-FRT-TO-eGFP-pICln,
5′-GGATCCATGAGCTTCCTCAAAAGTTTCCC-3′
and 5′-GTCTCGAGTCAGTGATCAACATCTGCATCC-3’;
pcDNA5-FRT-TO-eGFP-WD45,
5′-GGATCCATGCGGAAGGAAACCCCAC-3′
and 5′-GCGGCCGCCTACTCAGTAACACTTGCAGGTCC-3’.

Generation of pGEX-6P-1-PRMT5, pGEX-6P-1-WD45, pGEX-6P-1-RioK1 (Guderian et al. 2011), and pGEX-6P-1-pICln (Schmitz et al. 2021), and pcDNA5-FRT-TO-eGFP (Löffler et al. 2011) plasmids have been described previously.

Protein expression and purification

E. coli BL21 was transformed and grown overnight at 37 °C on selection plates (100 µg/mL ampicillin). 150 mL LB medium was inoculated and grown overnight at 37 °C. 1 L SB media (35 g/L Tryptone, 20 g/L Yeast extract, 5 g/L NaCl) culture was grown to an OD_{600} of 0.8. Protein expression was induced with 1 mM IPTG at 18 °C overnight. The bacteria were lysed in 300 mM Na

Cl, 50 mM Tris pH 7.5, 5 mM EDTA, 5 mM EGTA, 0.01% (v/v) Igepal, protease inhibitors (cOmplete Protease Inhibitor, 4693,132,001, Roche) and 50 mg/mL lysozyme. After sonication, lysates were centrifuged for 30 min at 10,000 g, incubated for 1.5 h at 4 °C with Glutathione-Sepharose 4B (Cytiva, 17,075,601), and washed three times with lysis buffer. The GST-tag was cleaved with PreScission Protease (Cytiva, 27,084,301) overnight at 4 °C.

The active PRMT5/WD45 complex was purchased from Active Motif (31,521). GFP-tagged proteins were expressed in HEK293 cells and purified by GFP-Trap Agarose (gta-20, Chromotek).

Antibodies

Primary antibodies: α-NF90 (A303-651A, Bethyl), α-PRMT5 (2252, CST), α-WD45 (2823, CST), α-RioK1 (NBP1-30103, Novus Biologicals), α-pICln (sc-393525, Santa Cruz), α-GFP (3H9, Chromotek). Secondary antibodies using LI-COR Odyssey Imaging System: IRDye 680LT goat α-rabbit, IRDye 680LT goat α-mouse, IRDye 800CW donkey α-rabbit, IRDye 800CW donkey α-mouse, IRDye 800CW goat α-rat (LI-COR Biosciences).

Cell culture and cell lines

HEK293 cells were cultured in high glucose DMEM (41,965,039, Gibco) with 10% (v/v) tetracycline-free FCS (10,270,106, Gibco) and 100 units/mL of Penicillin and 100 µg/mL Streptomycin (15,140,122, Gibco) in a 5% CO_2 atmosphere at 37 °C. Cells were washed with PBS (14,190,169, Gibco) and treated with Trypsin-EDTA (25,300,054, Gibco).

Inducible Flp-In T-REx 293 cell lines (R78007, Invitrogen), stably expressing NF90 wt, NF90 7x, GFP-NF90 wt, GFP-NF90 7x, GFP-PRMT5, GFP-WD45, GFP-pICln, and GFP-RioK1 were generated by co-transfecting 4.5 µg pOG44 and 0.5 µg pcDNA5 plasmids with FuGENE HD (E2311, Promega). Cells were selected with 200 µg/mL Hygromycin B Gold (ant-hg-1, Invivogen) and 5 µg/mL Blasticidin (ant-bl-05, Invivogen) for three weeks. GFP-pICln cells were generated as described in (Schmitz et al. 2021). Protein expression was induced with 0.1 µg/mL Doxycycline and cells were harvested after 24 h. For methylation inhibition 20 µM of the S-adenosylhomocysteine hydrolase inhibitor Adenosine Dialdehyde (Adox) (Cay15644, Cayman Chemical) was used.

Immunoprecipitation and immunoblotting

Cell lysates were generated using lysis buffer with 50 mM Tris pH 7.5, 150 mM NaCl, 1 mM EDTA, 1 mM EGTA, 1% Triton X-100 and 1x Protease inhibitor (P2714, Sigma–Aldrich). Protein concentration was measured by Bradford assay (5,000,006, Bio-Rad). 500 µg cell lysate was used for immunoprecipitation together with 1 µg of antibodies and Protein G Sepharose (17,061,801, Cytiva) at 4 °C for 1.5 h with rotation. As input 25 µg of total protein was loaded. GFP-tagged proteins were purified by GFP-Trap Agarose (gta-20, Chromotek) at 4 °C for 1.5 h with rotation. Samples were washed three times with washing buffer (lysis buffer without Triton X-100 and protease inhibitors) and eluted in sample buffer (375 mM Tris pH 7.5, 25.8% (w/v) glycerol, 12.3% (w/v) SDS, 0.06% (w/v) bromophenol blue, 6% (v/v) β-mercaptoethanol, pH 6.8). Subsequently, samples were separated by Tris/Glycine-SDS-PAGE and transferred to a PVDF membrane (Immobilon-FL, Merck Millipore). The immunoblot detection was carried out using the indicated primary and fluorescent-labeled secondary antibodies and the LI-COR Odyssey Imaging System.

In vitro methylation

Target proteins were incubated with 150 ng of Flag-PRMT5/WD45 from Sf9 cells (Active Motif, 31,521) and 1 µCi Adenosyl-L-Methionine, S-[methyl-3H] (Hartmann-Analytic, ART0288) in 50 mM Tris pH 7.5, 1 mM EGTA and 1 mM EDTA for 1.5 h at 37 °C. The reaction was stopped by adding sample buffer. Samples were separated by Tris/Glycine-SDS-PAGE and, after blotting and amido black staining (40% Methanol (v/v), 10% Acetic acid (v/v), 0.1% Amido black 10B (w/v)), analyzed by autoradiography with Amersham Hyperfilm MP (28,906,844, Cytiva) and BioMax TranScreen LE (1,622,034, Carestream).

Microscale thermophoresis

A Monolith NT 115 (NanoTemper Technologies) was used for microscale thermophoresis binding studies. Purified recombinant proteins GST-PRMT5, RioK1 or NF90 were labeled with AlexaFluor488-NHS (A20000, Invitrogen) in 50 mM HEPES, 300 mM NaCl, pH 7.5. 50 nM of labeled proteins and 4–14 µM of unlabeled proteins were used for interaction studies and measured as triplicates with 50% MST power and 50% LED power in premium or hydrophobic capillaries.

Acknowledgments: We also thank our colleagues David Schlütermann, Niklas Berleth, and Fabian Stuhldreier for their comments on the manuscript.

Author contributions: All the authors have accepted responsibility for the entire content of this submitted manuscript and approved submission.

Research funding: This work was supported by grants from Deutsche Forschungsgemeinschaft [RTG 2158 (to B.S. and S.W.), RTG 2578 (to B.S. and S.W.), and STO 864/4-3, STO 864/5-1, STO 864/6-1 (to B.S.)] and the Düsseldorf School of Oncology (funded by the Comprehensive Cancer Center Düsseldorf/Deutsche Krebshilfe and the Medical Faculty of the Heinrich Heine University Düsseldorf; to B.S. and S.W.).

Conflict of interest statement: The authors declare no conflicts of interest regarding this article.

References

Antonysamy, S., Bonday, Z., Campbell, R.M., Doyle, B., Druzina, Z., Gheyi, T., Han, B., Jungheim, L.N., Qian, Y., Rauch, C., et al. (2012). Crystal structure of the human PRMT5:MEP50 complex. Proc. Natl. Acad. Sci. U.S.A. 109: 17960–17965.

Bedford, M.T. and Clarke, S.G. (2009). Protein arginine methylation in mammals: who, what, and why. Mol. Cell 33: 1–13.

Blanc, R.S. and Richard, S. (2017). Arginine methylation: the coming of age. Mol. Cell 65: 8–24.

Bottger, A., Islam, M.S., Chowdhury, R., Schofield, C.J., and Wolf, A. (2015). The oxygenase Jmjd6–a case study in conflicting assignments. Biochem. J. 468: 191–202.

Chan-Penebre, E., Kuplast, K.G., Majer, C.R., Boriack-Sjodin, P.A., Wigle, T.J., Johnston, L.D., Rioux, N., Munchhof, M.J., Jin, L., Jacques, S.L., et al. (2015). A selective inhibitor of PRMT5 with in vivo and in vitro potency in MCL models. Nat. Chem. Biol. 11: 432–437.

Chang, B., Chen, Y., Zhao, Y., and Bruick, R.K. (2007). JMJD6 is a histone arginine demethylase. Science 318: 444–447.

Chari, A., Golas, M.M., Klingenhager, M., Neuenkirchen, N., Sander, B., Englbrecht, C., Sickmann, A., Stark, H., and Fischer, U. (2008).

An assembly chaperone collaborates with the SMN complex to generate spliceosomal SnRNPs. Cell 135: 497–509.

Chen, D.H., Wu, K.T., Hung, C.J., Hsieh, M., and Li, C. (2004). Effects of adenosine dialdehyde treatment on *in vitro* and *in vivo* stable protein methylation in HeLa cells. J. Biochem. 136: 371–376.

Guderian, G., Peter, C., Wiesner, J., Sickmann, A., Schulze-Osthoff, K., Fischer, U., and Grimmler, M. (2011). RioK1, a new interactor of protein arginine methyltransferase 5 (PRMT5), competes with pICln for binding and modulates PRMT5 complex composition and substrate specificity. J. Biol. Chem. 286: 1976–1986.

Hadjikyriacou, A., Yang, Y., Espejo, A., Bedford, M.T., and Clarke, S.G. (2015). Unique features of human protein arginine methyltransferase 9 (PRMT9) and its substrate RNA splicing factor SF3B2. J. Biol. Chem. 290: 16723–16743.

Han, G., Li, J., Wang, Y., Li, X., Mao, H., Liu, Y., and Chen, C.D. (2012). The hydroxylation activity of Jmjd6 is required for its homo-oligomerization. J. Cell. Biochem. 113: 1663–1670.

Herrmann, F., Bossert, M., Schwander, A., Akgun, E., and Fackelmayer, F.O. (2004). Arginine methylation of scaffold attachment factor A by heterogeneous nuclear ribonucleoprotein particle-associated PRMT1. J. Biol. Chem. 279: 48774–48779.

Krzyzanowski, A., Gasper, R., Adihou, H., Hart, P.T., and Waldmann, H. (2021). Biochemical investigation of the interaction of pICln, RioK1 and COPR5 with the PRMT5-MEP50 complex. Chembiochem 22: 1908–1914.

Lapeyre, B., Amalric, F., Ghaffari, S.H., Rao, S.V., Dumbar, T.S., and Olson, M.O. (1986). Protein and cDNA sequence of a glycine-rich, dimethylarginine-containing region located near the carboxyl-terminal end of nucleolin (C23 and 100 kDa). J. Biol. Chem. 261: 9167–9173.

Lischwe, M.A., Ochs, R.L., Reddy, R., Cook, R.G., Yeoman, L.C., Tan, E.M., Reichlin, M., and Busch, H. (1985). Purification and partial characterization of a nucleolar scleroderma antigen (Mr = 34, 000; pI, 8.5) rich in NG, NG-dimethylarginine. J. Biol. Chem. 260: 14304–14310.

Lischwe, M.A., Roberts, K.D., Yeoman, L.C., and Busch, H. (1982). Nucleolar specific acidic phosphoprotein C23 is highly methylated. J. Biol. Chem. 257: 14600–14602.

Liu, W., Ma, Q., Wong, K., Li, W., Ohgi, K., Zhang, J., Aggarwal, A., and Rosenfeld, M.G. (2013). Brd4 and JMJD6-associated anti-pause enhancers in regulation of transcriptional pause release. Cell 155: 1581–1595.

Löffler, A.S., Alers, S., Dieterle, A.M., Keppeler, H., Franz-Wachtel, M., Kundu, M., Campbell, D.G., Wesselborg, S., Alessi, D.R., and Stork, B. (2011). Ulk1-mediated phosphorylation of AMPK constitutes a negative regulatory feedback loop. Autophagy 7: 696–706.

Mckinney, D.C., Mcmillan, B.J., Ranaghan, M.J., Moroco, J.A., Brousseau, M., Mullin-Bernstein, Z., O'keefe, M., Mccarren, P., Mesleh, M.F., Mulvaney, K.M., et al. (2021). Discovery of a first-in-class inhibitor of the PRMT5-substrate adaptor interaction. J. Med. Chem. 64: 11148–11168.

Mulvaney, K.M., Blomquist, C., Acharya, N., Li, R., Ranaghan, M.J., O'keefe, M., Rodriguez, D.J., Young, M.J., Kesar, D., Pal, D., et al. (2021). Molecular basis for substrate recruitment to the PRMT5 methylosome. Mol. Cell 81: 3481–3495.e7.

Murn, J. and Shi, Y. (2017). The winding path of protein methylation research: milestones and new frontiers. Nat. Rev. Mol. Cell Biol. 18: 517–527.

Musiani, D., Bok, J., Massignani, E., Wu, L., Tabaglio, T., Ippolito, M.R., Cuomo, A., Ozbek, U., Zorgati, H., Ghoshdastider, U., et al. (2019). Proteomics profiling of arginine methylation defines PRMT5 substrate specificity. Sci. Signal. 12, https://doi.org/10.1126/scisignal.aat8388.

Pal, S., Vishwanath, S.N., Erdjument-Bromage, H., Tempst, P., and Sif, S. (2004). Human SWI/SNF-associated PRMT5 methylates histone H3 arginine 8 and negatively regulates expression of ST7 and NM23 tumor suppressor genes. Mol. Cell Biol. 24: 9630–9645.

Pollack, B.P., Kotenko, S.V., He, W., Izotova, L.S., Barnoski, B.L., and Pestka, S. (1999). The human homologue of the yeast proteins Skb1 and Hsl7p interacts with Jak kinases and contains protein methyltransferase activity. J. Biol. Chem. 274: 31531–31542.

Poulard, C., Rambaud, J., Hussein, N., Corbo, L., and Le Romancer, M. (2014). JMJD6 regulates ERalpha methylation on arginine. PLoS One 9: e87982.

Richard, S., Morel, M., and Cleroux, P. (2005). Arginine methylation regulates IL-2 gene expression: a role for protein arginine methyltransferase 5 (PRMT5). Biochem. J. 388: 379–386.

Schmitz, K., Cox, J., Esser, L.M., Voss, M., Sander, K., Loffler, A., Hillebrand, F., Erkelenz, S., Schaal, H., Kahne, T., et al. (2021). An essential role of the autophagy activating kinase ULK1 in snRNP biogenesis. Nucleic Acids Res 49: 6437–6455.

Simms, S.A., Stock, A.M., and Stock, J.B. (1987). Purification and characterization of the S-adenosylmethionine:glutamyl methyltransferase that modifies membrane chemoreceptor proteins in bacteria. J. Biol. Chem. 262: 8537–8543.

Tsai, W.C., Reineke, L.C., Jain, A., Jung, S.Y., and Lloyd, R.E. (2017). Histone arginine demethylase JMJD6 is linked to stress granule assembly through demethylation of the stress granule-nucleating protein G3BP1. J. Biol. Chem. 292: 18886–18896.

Wandrey, F., Montellese, C., Koos, K., Badertscher, L., Bammert, L., Cook, A.G., Zemp, I., Horvath, P., and Kutay, U. (2015). The NF45/NF90 heterodimer contributes to the biogenesis of 60S ribosomal subunits and influences nucleolar morphology. Mol. Cell Biol. 35: 3491–3503.

Webby, C.J., Wolf, A., Gromak, N., Dreger, M., Kramer, H., Kessler, B., Nielsen, M.L., Schmitz, C., Butler, D.S., Yates, J.R., 3rd, et al. (2009). Jmjd6 catalyses lysyl-hydroxylation of U2AF65, a protein associated with RNA splicing. Science 325: 90–93.

Widmann, B., Wandrey, F., Badertscher, L., Wyler, E., Pfannstiel, J., Zemp, I., and Kutay, U. (2012). The kinase activity of human Rio1 is required for final steps of cytoplasmic maturation of 40S subunits. Mol. Biol. Cell 23: 22–35.

Supplementary Material: The online version of this article offers supplementary material (https://doi.org/10.1515/hsz-2022-0136).